

RHIC Dipole Cold Mass Patch Weld Evaluation

S. Kane

March 1995

Collider Accelerator Department
Brookhaven National Laboratory

U.S. Department of Energy

USDOE Office of Science (SC)

Notice: This technical note has been authored by employees of Brookhaven Science Associates, LLC under Contract No. DE-AC02-76CH00016 with the U.S. Department of Energy. The publisher by accepting the technical note for publication acknowledges that the United States Government retains a non-exclusive, paid-up, irrevocable, world-wide license to publish or reproduce the published form of this technical note, or allow others to do so, for United States Government purposes.

DISCLAIMER

This report was prepared as an account of work sponsored by an agency of the United States Government. Neither the United States Government nor any agency thereof, nor any of their employees, nor any of their contractors, subcontractors, or their employees, makes any warranty, express or implied, or assumes any legal liability or responsibility for the accuracy, completeness, or any third party's use or the results of such use of any information, apparatus, product, or process disclosed, or represents that its use would not infringe privately owned rights. Reference herein to any specific commercial product, process, or service by trade name, trademark, manufacturer, or otherwise, does not necessarily constitute or imply its endorsement, recommendation, or favoring by the United States Government or any agency thereof or its contractors or subcontractors. The views and opinions of authors expressed herein do not necessarily state or reflect those of the United States Government or any agency thereof.

AD/RHIC/RD-86

RHIC PROJECT
Brookhaven National Laboratory

RHIC Dipole Coldmass Patch Weld Evaluation

S.Kane, A. Farland, M. Anerella

March 1995

RHIC Dipole Coldmass Patch Weld Evaluation

S. Kane, A. Farland, M. Anerella

Abstract

The Coldmass Patch weld in the RHIC Dipole Magnet is a fillet weld attaching a circular cover over the tooling holes in the coldmass shells. These welds were found undersized on the first 30 magnets manufactured by Grumman. Subsequent inspection found the weld concavity to be as great as 0.050 inches for a specified 3/16 inch fillet. A test sample was manufactured to the worst case dimensions observed on delivered magnets. The test sample was instrumented using strain gauges and dial indicators, then hydraulically pressurized in conformance with the ASME Boiler & Pressure Vessel Code. Testing was discontinued at 6,000 psi without failure of the test specimen. The test data shows the non-conforming weld meets ASME Boiler & Pressure Vessel Code requirements.

Background

The RHIC Dipole Magnet Coldmass shells have 22 holes through which tooling is placed to mechanically locate the magnet laminations during assembly and welding. These holes are subsequently sealed using circular disks, or patches, conforming to the curvature of the coldmass shells, and fillet welds using the RHIC-specific weld alloy. The stress in the weld is a function of the patch diameter, and the welds are critically loaded in this application for RHIC. In fact, the initial design was changed via ECN 469 to a round patch, 2.1 inches in diameter to ensure compliance with the American Society of Mechanical Engineers (ASME) Boiler & Pressure Vessel Code. Inspection of some patch welds on initial Grumman-manufactured magnets revealed unacceptable concavity and size. This was not completely corrected until Phase Two magnet DRG-503.

The BNL drawings and the Dipole contract require conformance with the ASME Boiler and Pressure Vessel Code. Section IX, *Qualification Standard for Welding and Brazing Procedures, Welders, Brazers, and Welding and Brazing Operators*, Paragraph QW-491, General, states:

“Definition of the more common terms relating to welding are defined in QW-492. These are in substantial agreement with the definitions of the American Welding Society given in their document, AWS A 3.0-76, Terms and Definitions.”

Paragraph QW-492, Definitions, provides the following definition:

“size of weld, fillet weld: for equal leg fillet welds — the leg lengths of the largest isosceles right triangle which can be inscribed within the fillet-weld cross section”

This definition is identical with that of ANSI/AWS A3.0-89, *Standard Welding Terms and Definitions*, and the size of a fillet weld and weld concavity are graphically depicted in Figure 1. The concavity of the coldmass patch welds on the delivered Grumman dipole magnets clearly reduces the size of the weld used in engineering calculations, and this weld is already critically stressed, seeing 98% of the allowable limit at the design internal pressure of 275 psi. Therefore, any reduction in fillet weld size due to concavity would result in calculated stresses beyond the allowable limit.

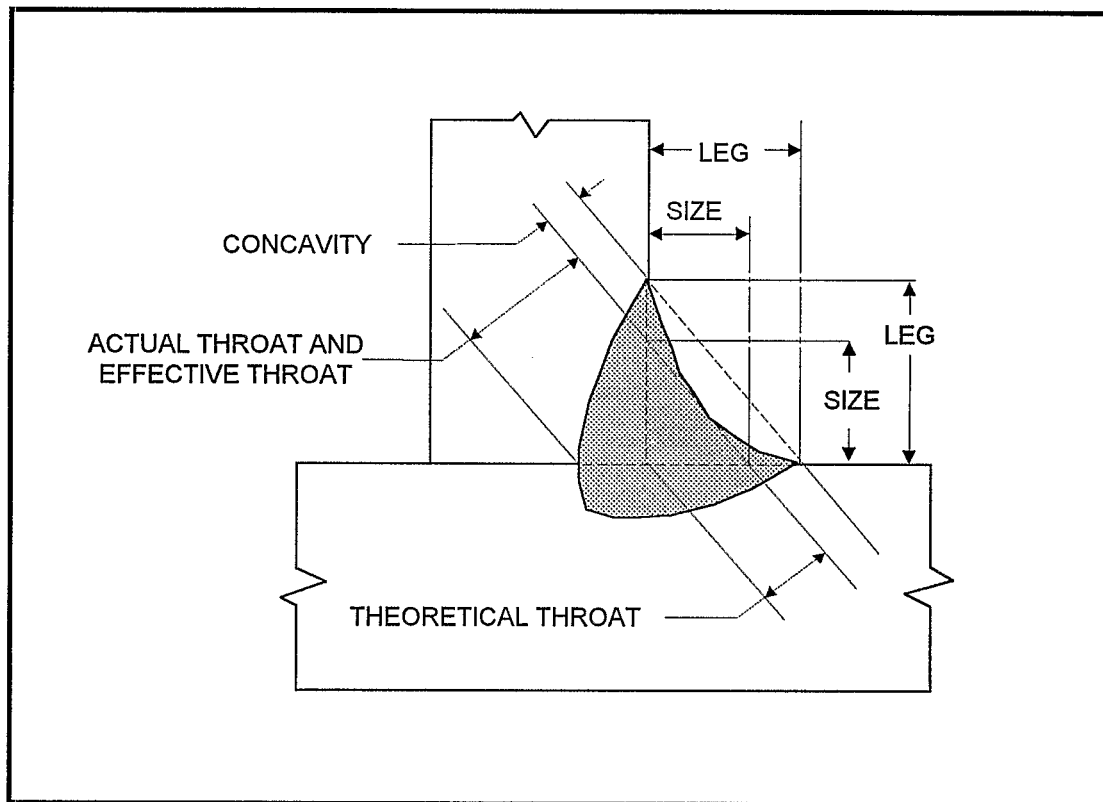


Figure 1. Fillet Weld Nomenclature

The issue to be addressed became the acceptability of the non-conforming welds on the delivered magnets. Further analysis becomes very difficult at this small scale. However, the ASME Boiler & Pressure Vessel Code provides empirical methods to establish allowable pressure. Specifically, Section VIII, Division 1, *Rules for Construction of Pressure Vessels*, Paragraph UG-101, Proof Tests to Establish Maximum Allowable Working Pressure, provides two types of tests to determine the internal maximum allowable working pressure — tests based upon material yielding and tests based upon bursting of the part. The tests based upon material yielding are prescribed by paragraphs UG-101(l), (n), and (o). These are:

- UG-101(l) Brittle-Coating Test Procedure - the parts to be tested are coated with a brittle coating. Pressure is applied and released incrementally, until the coating begins flaking or strain lines appear.

- UG-101(n) Strain Measurement Test Procedure - strain gages are attached at the most highly stressed location of the part. Pressure is applied and released incrementally, until the strains reach 0.2% permanent strain.
- UG-101(o) Displacement Measurement Test Procedure - devices capable of measuring to 0.001 inches shall be used to measure displacement at the most highly stressed location. Pressure is applied and released incrementally, until the plot of displacement under pressure deviates from a straight line.

Maximum allowable working pressure is then calculated by

$$P = 0.5 \times H \times \frac{S_y}{S_{y \text{ avg}}} \quad \text{or} \quad P = 0.4 \times H$$

where

H = hydrostatic test pressure when test was stopped
 S_y = specified minimum yield strength
 S_{y avg} = average actual yield strength

The second formula is used if the actual average yield strength is not determined by test specimens.

The test based upon bursting of the part is prescribed by UG-101(m). Hydrostatic pressure is increased until the part bursts. Maximum allowable working pressure is then calculated by

$$P = \frac{B}{5} \times \frac{S_{\mu} E}{S_{\mu \text{ avg}}} \quad \text{or} \quad P = \frac{B}{5} \times \frac{S_{\mu} E}{S_{\mu r}}$$

where

B = bursting test pressure
 E = weld joint efficiency
 S_μ = specified minimum tensile strength
 S_{μ avg} = average actual tensile strength
 S_r = maximum actual tensile strength of range of specification

Procedure

A proof test of an article representing the worst case weld configuration for the delivered magnets would address all non-conforming magnets. All delivered magnets not in test were inspected by E. Jochen, Central Shops Weld Inspector, using a custom 3/16" fillet weld gage set, especially manufactured by Central Shops to measure concavity. The gages were produced to measure concavity of 0.000", 0.010", 0.020", 0.030", 0.040", and 0.050". However, only eight of the 22 patches can be inspected. These patches, four at each end, are located on the ends of the coldmass protruding from the cryostat. The remainder are wrapped with super-insulation and access is blocked by the cryostat. The measurements are listed in Appendix A. No welds were found to measure less than 3/16", and the concavity measured was not greater than 0.050".

A test specimen was prepared using 3 inch diameter, 4 inch long Type 304 round bar stock and a RHIC Dipole coldmass patch. A blind hole was bored axially in the center of the bar stock to form a pressure cavity, and another hole was bored radially to communicate with that cavity and threaded to accept a 3/8" Swage-Lok fitting. The patch was flattened and welded to the end of the pressure cavity using the RHIC specific weld alloy, RHIC-MAG-M-4360. The specimen was assembled for welding, and back-purged with 99.99% pure Argon at a rate of 5 cubic feet per hour (CFH) for a minimum of five minutes. Gas Tungsten Arc Welding (GTAW) was performed using a 3/32 inch, 2% thoriated tungsten electrode and 50 to 150 amperes of DC current. Shield gas was 99.99% pure Argon flowing at a rate of 15 CFH through a Number 6 gas cup. Back-purging was maintained for a minimum of five minutes after welding was completed. The finished weld was a 3/16" fillet weld with 0.050" concavity all around. The concavity was measured by E. Jochen.

The patch was instrumented using eight model WK-06-125AD 0.35" strain gages with a gage factor of 2.07 wired in quarter bridge mode through V/E-21 gage terminal blocks and V/E-21 switch and balance unit to a V/E-20 digital strain indicator. The gage locations are shown in Figure 2. The test article was restrained on a steel table using an ENERPAC jack installed in a press fixture. An ENERPAC Model P-39 hydraulic hand pump with a 10,000 psi capacity was connected to the test article using steel tubing. A Starrett dial indicator with 0.001" increments was installed to measure the displacement at the center of the patch. This measurement was referenced by a second dial indicator installed at the base of the test article.

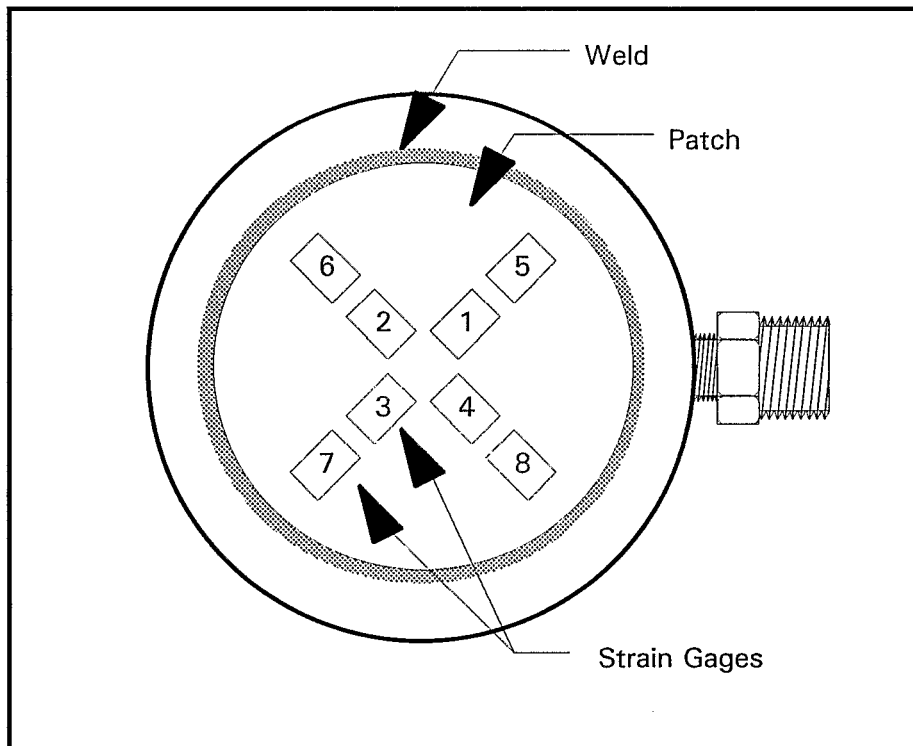


Figure 2. Strain Gage Location

The ultimate objective of the test was to burst the part. However, instrumentation was applied to capture data for evaluation using the other tests based upon material yielding, and to evaluate the different methods for similar testing of another design. The strain gages were calibrated immediately preceding the test. The general procedure followed was to apply pressure, record strain gage and dial indicator readings, then release the pressure and, again, record strain gage and dial indicator readings. The initial pressure was the design pressure, 275 psi. The next pressure level was 400 psi, and subsequent pressure levels were increased in 200 psi increments, until 3,200 psi. At this point, the centrally located strain gage instrumentation was lost. Subsequent pressure levels were increased in increments of 400 psi to hasten the test. The outer strain gage instrumentation was lost after 4,800 psi. The test was stopped after 6,000 psi, without having burst the part. The data collected is tabulated in Appendix B.

Results and Discussion

It was not possible to mount strain gages on the weld. Strain gages were mounted as close to the center of the test article and as near the weld as possible. These indications must be projected to the stresses on the weld. Mathematical modeling of the stresses and strains in the patch is limited to lower pressures by the elastic limits of the material. Using conventional formulae for circular flat plates and assuming fixed end conditions, the greatest stresses are located at the welds. These stresses are 55% greater than the stresses at the center of the patch, and 70% to 210% greater than the strain gage indications. The calculations for the model are provided in Appendix C.

Evaluation of Results using Strain Gage Method

UG-101(n), Strain Measurement Test Procedure, subparagraph (3) requires two curves of the strain versus the test pressure be plotted for each gage, one showing strain under pressure and the second showing permanent strain when the pressure is removed. These plots are shown in Figures 3 and 4. However, the strain gages are slightly displaced from the location of highest stress. These strains were corrected to reflect the higher values for the nearest high stress area determined by the mathematical model, and are shown in Figures 5 and 6. Table 2 shows the correction factors. Gages #1 through #4 were corrected to reflect the strain at the center, and gages #5 through #8 were corrected to reflect the strains at the weld. Figure 6 shows the 0.2% permanent strain (2000 microstrain) at the center of the patch is exceeded at a pressure of 3,000 psi. This pressure is lower than the pressure at which the permanent strain at the welds exceeds 0.2%. Therefore, the greatest pressure the part sustained without exceeding 0.2% strain is 2,800 psi.

Table 2
Correction Factors for Strain Gage Location

Strain Gage	#1	#2	#3	#4	#5	#6	#7	#8
Correction Factor	1.231	1.108	1.177	1.177	2.452	3.107	2.379	2.011

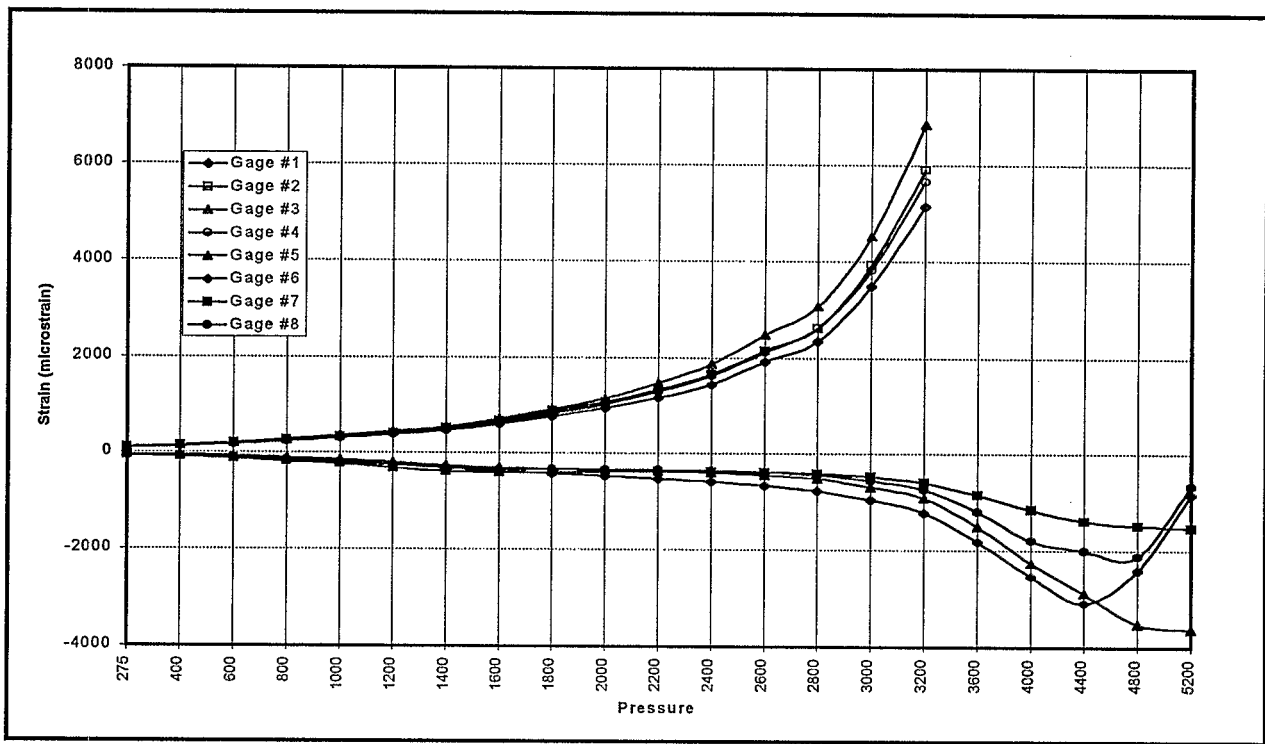


Figure 3. Strain Gage Data While Pressurized

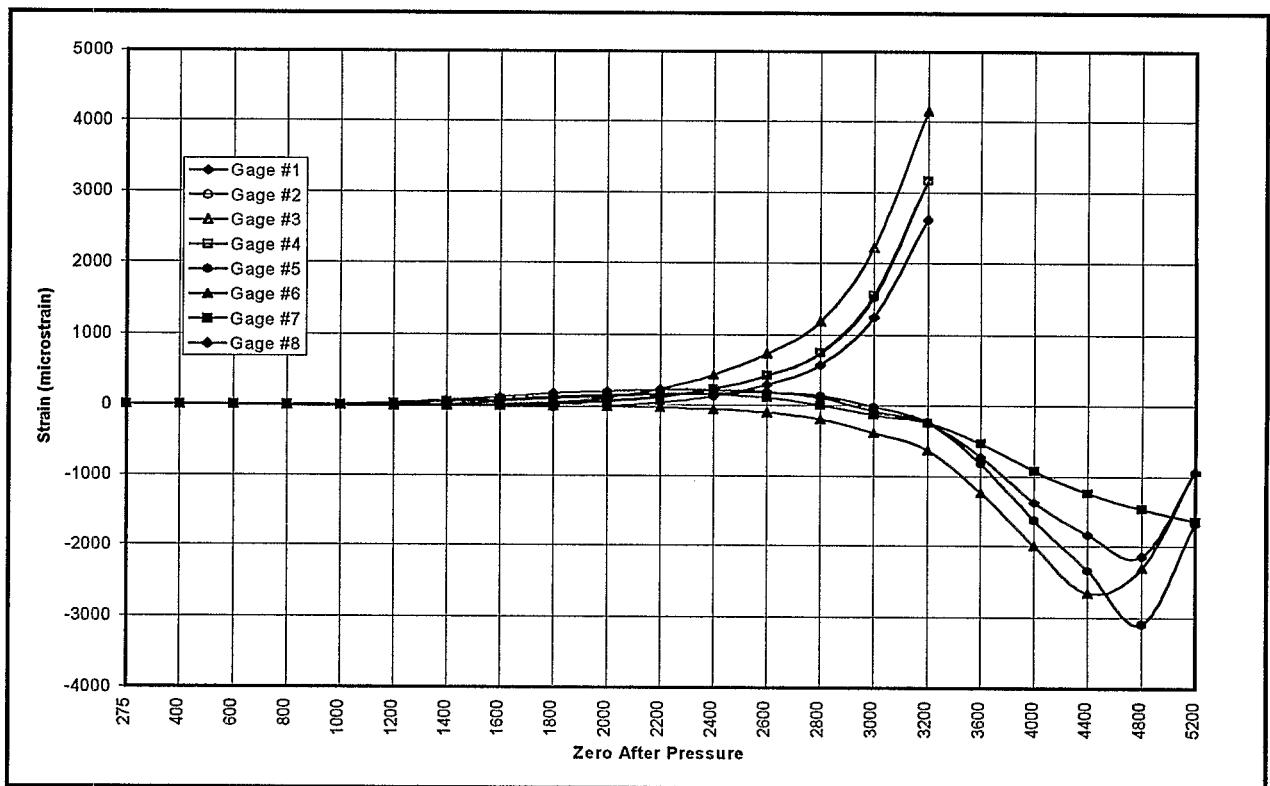


Figure 4. Strain Gage Data After Pressurization (Depressurized)

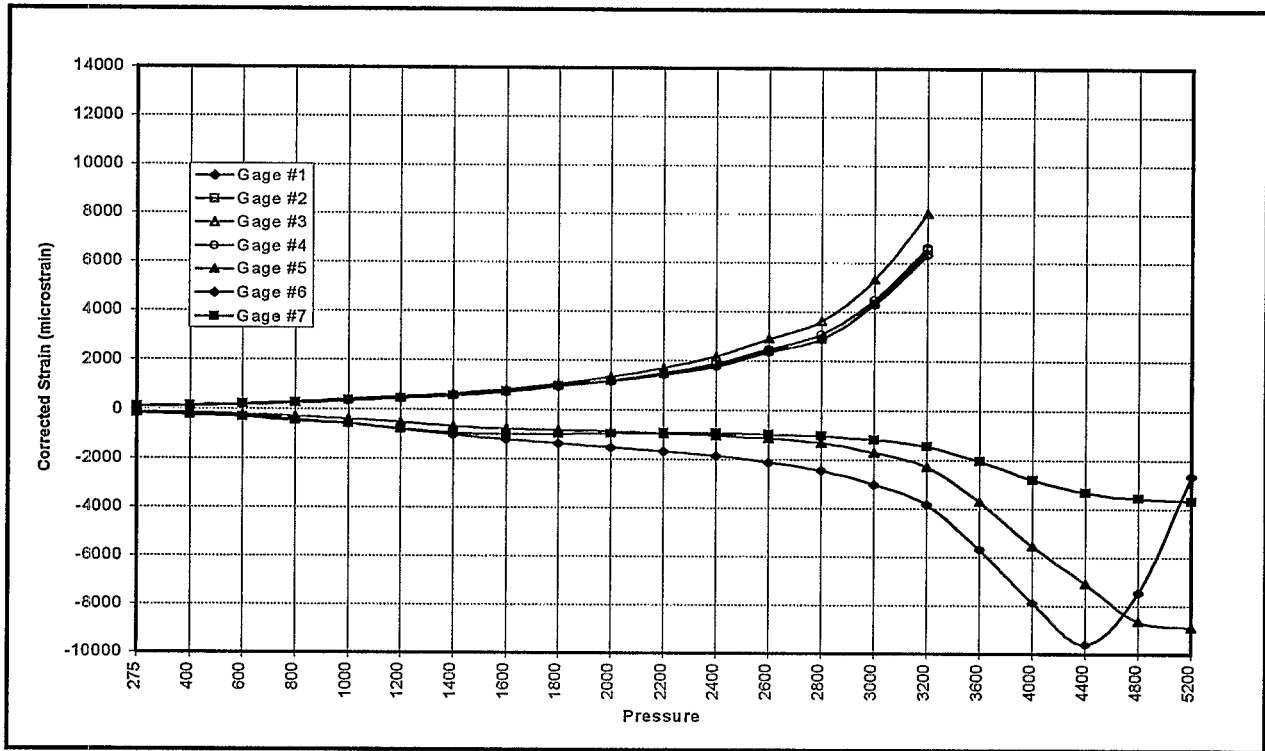


Figure 5. Corrected Strain Gage Data While Pressurized

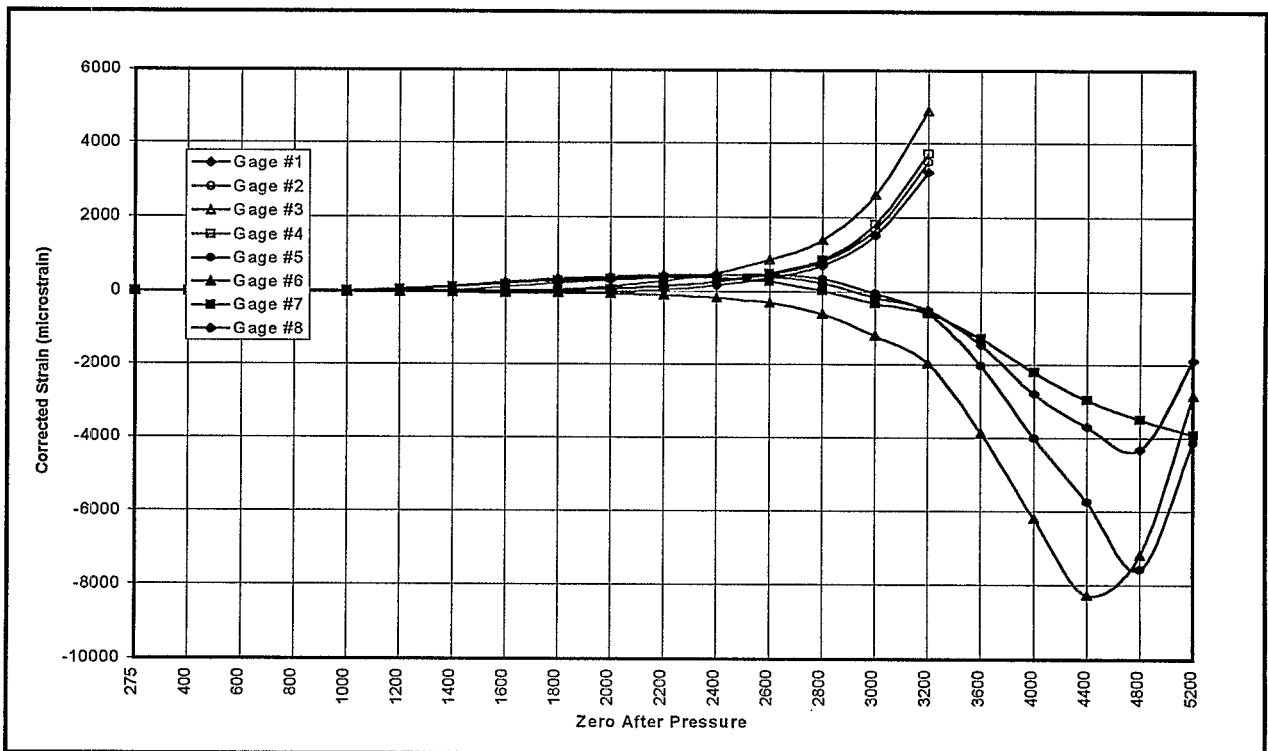


Figure 6. Corrected Strain Gage Data After Pressurization (Depressurized)

The part is too small to make tensile specimens for determination of actual yield strength. The heat number or other identification of the plate origin is not known, hence it is not possible to make tensile specimens of the same material. This requires use of the following equation for determination of the maximum allowable working pressure:

$$P = 0.4 \times H$$

Thus the maximum allowable working pressure for the coldmass patch using the ASME Strain Measurement Test Procedure for Proof Tests to Establish Maximum Allowable Working Pressure is 1,120 psi.

Evaluation of Results using Displacement Measurement Method

The dial indicator indexing the patch was located at the center. Figure 6 above shows the center of the patch was the most highly stressed location of this part, satisfying the requirement of UG-101(o), Displacement Measurement Test Procedure, subparagraph (1), for location of the indicators. UG-101(o), Displacement Measurement Test Procedure, subparagraph (3) requires two curves of the displacement versus the test pressure be plotted for each reference point — one plot is of the displacement under pressure, the other shows permanent displacement when pressure is removed. Pressure is applied and released incrementally, until the plot of displacement under pressure deviates from a straight line. These plots are shown in Figure 7.

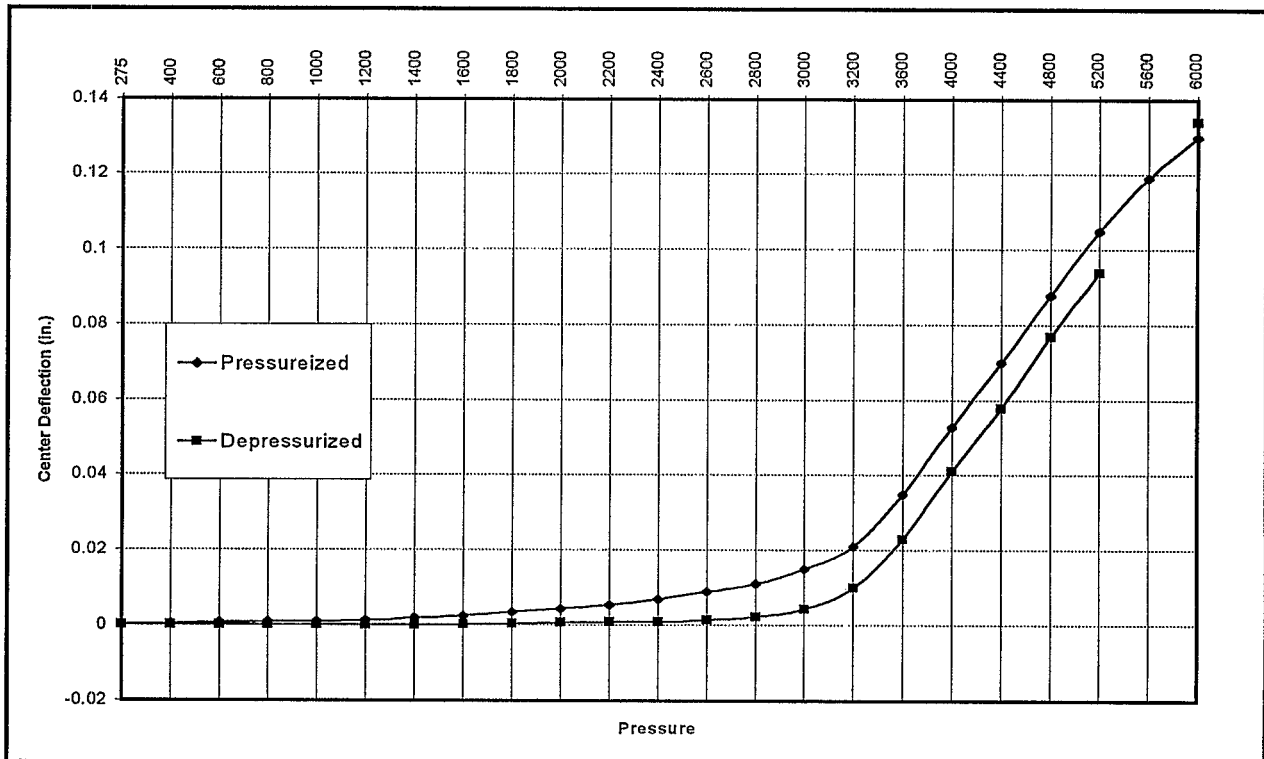


Figure 7. Displacement Data Plot

The plot of displacement under pressure departs from a straight line beyond 1,200 psi. As in the strain gage method, the maximum allowable working pressure is defined by:

$$P = 0.4 \times H$$

Thus the maximum allowable working pressure for the coldmass patch using the ASME Displacement Measurement Test Procedure of UG-101, Proof Tests to Establish Maximum Allowable Working Pressure, is 480 psi.

Evaluation of Results using Burst Method

The part did not burst during testing. However, the part did achieve 6,000 psi. Using this value as the burst pressure would be a conservative, and safe, assumption. The only problem in using the Burst Method equation for determination of Maximum Allowable Working Pressure is that it requires the average actual tensile strength of the test specimen or the maximum tensile strength of the range of the specification. ASME's own material specification, SA-240, does not specify a maximum tensile strength, and it is not possible to determine the actual tensile strength of the test parts. Studies¹ have found that the average tensile strength for Type 304 stainless steel at room temperature is approximately 100,000 psi. Using this value in the Burst Method equation, the ASME specification SA-240 minimum tensile strength of 75,000 psi, and the ASME Section VIII, Division 1, Table UW-12 Joint Efficiency value of 0.45 for a single full fillet weld, the maximum allowable working pressure is 378 psi. This number has significant conservatism built in for the following reasons:

1. actual burst pressure is greater than 6,000 psi,
2. The formula uses a factor of safety of 5,
3. the assumed average tensile strength for Type 304 stainless steel is 43% greater than the minimum specified tensile strength, and
4. the joint efficiency increases the safety factor to over 11.

Assessment of the Test Results

The three test methods used in this procedure produced different results, yielding maximum allowable working pressures from 1,120 psi to 378 psi. However, the magnitude of the maximum allowable working pressures were directly related to the degree of accuracy of the test instrumentation. The results were more conservative for less exacting measures of component stress. These results indicate the values determined by displacement are more conservative than direct measurement of actual strain.

The disparity in the test results may cause speculation about "over design." The ASME requirements use yield strength as the criterion for material limits. This is sufficiently true for most engineering materials. However, material characteristics, hence their analytical techniques, are not predictable beyond the proportional limit of their yield strengths. For this case where

¹ Mechanical and Physical Properties of the Austenitic Chromium-Nickel Stainless Steels at Subzero Temperatures; The International Nickel Company, Inc., 3rd Edition, 1970

Type 304 austenitic stainless steels are used, their yield strengths are just 30,000 psi, compared with their ultimate strengths of 75,000, for a ratio of 1:2.5. Few other practical engineering materials for pressure vessels have this characteristic. Thus, the rules are designed to accommodate the majority of materials used, while erring on the side of conservatism for other materials. The ASME recognizes these issues, and provides other methods, such as the proof tests used here, to determine a component's safe maximum allowable working pressure.

Additionally, the ASME requirements use the minimum specified yield strength as the benchmark for material limits. These limits are derived from the worst case yield strengths within the material's specified chemical composition range. In practice, these materials exceed these values by at least 10%. Finally, the RHIC-specific weld alloy, RHIC-MAG-M-4360, is a new generation of cryogenic pressure vessel superalloys. While developed primarily for superior notch toughness at 4°K, it possesses superior yield strength. BNL testing shows its room temperature yield strength to be between 44 and 50 ksi — as much as 67% greater than the base material minimum specified yield strength. The success of this proof test is attributed to the exceptional properties of this weld alloy and not “over design.”

Conclusions

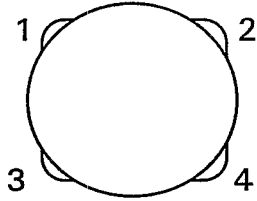
The Grumman Dipole coldmass patch welds with up to 0.050” concavity satisfy the requirements of the ASME Boiler & Pressure Vessel Code for the RHIC design maximum allowable working pressure of 275 psi.

APPENDIX A

RHIC Grumman Dipole

Coldmass Patch Fillet Weld Concavity

RHIC Grumman Dipole
Coldmass Patch Fillet Weld Concavity



Coldmass Patch Location

Magnet Serial No.	Lead End				Non-Lead End			
	1	2	3	4	1	2	3	4
DRG 101	0.030	0.040	0.050	0.050	0.030	0.040	0.040	0.040
DRG 102	0.030	0.030	0.030	0.040	0.030	0.010	0.040	0.030
DRG 103	0.030	0.020	0.040	0.030	0.040	0.040	0.040	0.040
DRG 104	0.050	0.050	0.050	0.030	0.040	0.040	0.040	0.040
DRG 105	0.050	0.050	0.050	0.050	0.040	0.020	0.040	0.030
DRG 106	0.040	0.030	0.040	0.040	0.030	0.030	0.040	0.030
DRG 107	0.040	0.050	0.050	0.050	0.040	0.030	0.050	0.040
DRG 108	0.050	0.050	0.050	0.050	0.040	0.020	0.040	0.040
DRG 109	0.040	0.020	0.050	0.050	0.030	0.040	0.050	0.050
DRG 110	0.040	0.050	0.050	0.050	0.050	0.040	0.020	0.030
DRG 111	0.030	0.030	0.050	0.030	0.040	0.040	0.030	0.030
DRG 112	0.040	0.040	0.050	0.040	0.040	0.040	0.040	0.040
DRG 113	0.030	0.040	0.030	0.020	0.030	0.030	0.030	0.020
DRG 114	0.020	0.020	0.030	0.040	0.030	0.030	0.030	0.050
DRG 115	0.020	0.030	0.040	0.020	OK	0.030	0.030	0.030
DRG 116	0.020	0.020	0.020	0.020	0.020	0.030	0.020	0.040
DRG 117	0.040	0.040	0.040	0.030	0.010	0.020	0.020	0.040
DRG 118	0.040	0.040	0.040	0.030	0.030	0.030	0.030	0.030
DRG 119	0.030	0.020	0.020	0.040	0.030	OK	0.020	0.020
DRG 123	0.030	0.030	0.030	0.030	0.040	0.040	0.010	0.030
DRG 124	0.030	OK	0.020	0.020	0.040	0.030	0.030	0.030
DRG 125	0.030	0.020	0.020	0.030	0.030	0.020	0.020	0.020
DRG 126	0.030	0.030	0.030	0.030	0.030	0.020	0.010	0.040
DRG 127	0.020	0.030	0.020	OK	0.030	0.020	OK	OK
DRG 128	0.030	0.030	0.020	0.030	0.010	OK	0.010	0.040
DRG 129	OK	OK	OK	OK	0.020	OK	OK	OK
DRG 130	OK	OK	OK	OK	OK	OK	0.020	OK
DRG 501	0.050	0.050	0.040	0.020	0.050	0.050	0.050	0.040
DRG 502	0.030	0.030	0.030	OK	0.040	0.020	0.040	0.020
DRG 503	OK	OK	OK	OK	OK	OK	OK	OK

APPENDIX B
RHIC Grumman Dipole
Coldmass Patch Fillet Weld
Proof Test Data

[illegible]

APPENDIX C

RHIC Grumman Dipole

Coldmass Patch Fillet Weld

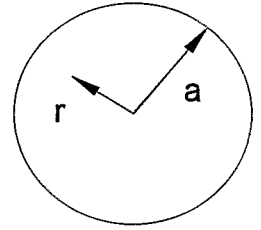
Mathematical Models

Analysis of Dipole Coldmass Patch Proof Test

$$\nu := 0.29 \quad t := \frac{3}{16} \cdot \text{in} \quad q := 275 \cdot \text{psi} \quad a := \frac{2.1}{2} \cdot \text{in} \quad r := 0 \cdot \text{in} \quad E := 29 \cdot 10^6 \cdot \text{psi}$$

$$D := \frac{E \cdot t^3}{12 \cdot (1 - \nu^2)} \quad D = 17392.92 \cdot \text{lbf} \cdot \text{in}$$

The disk has radius 'a'. Functions are measured from the center; 'c' is the center, 'a' is the outer edge, and 'r' is a point in between.



Fixed Edges

$$y_{cfe} := \frac{-a^4}{64 \cdot D} \quad *q \quad y_{cfe} = -1.092 \cdot 10^{-6} \cdot \frac{\text{in}}{\text{psi}} \quad *q \quad y_{cfe}(q) := \frac{-a^4}{64 \cdot D} \cdot q \quad y_{cfe}(q) = 0 \cdot \text{in}$$

$$M_{cfe} := \frac{a^2 \cdot (1 + \nu)}{16} \quad *q \quad M_{cfe} = 0.089 \cdot \text{in}^2 \quad *q \quad M_{cfe}(q) := \frac{a^2 \cdot (1 + \nu)}{16} \cdot q \quad M_{cfe}(q) = 24.444 \cdot \text{lbf}$$

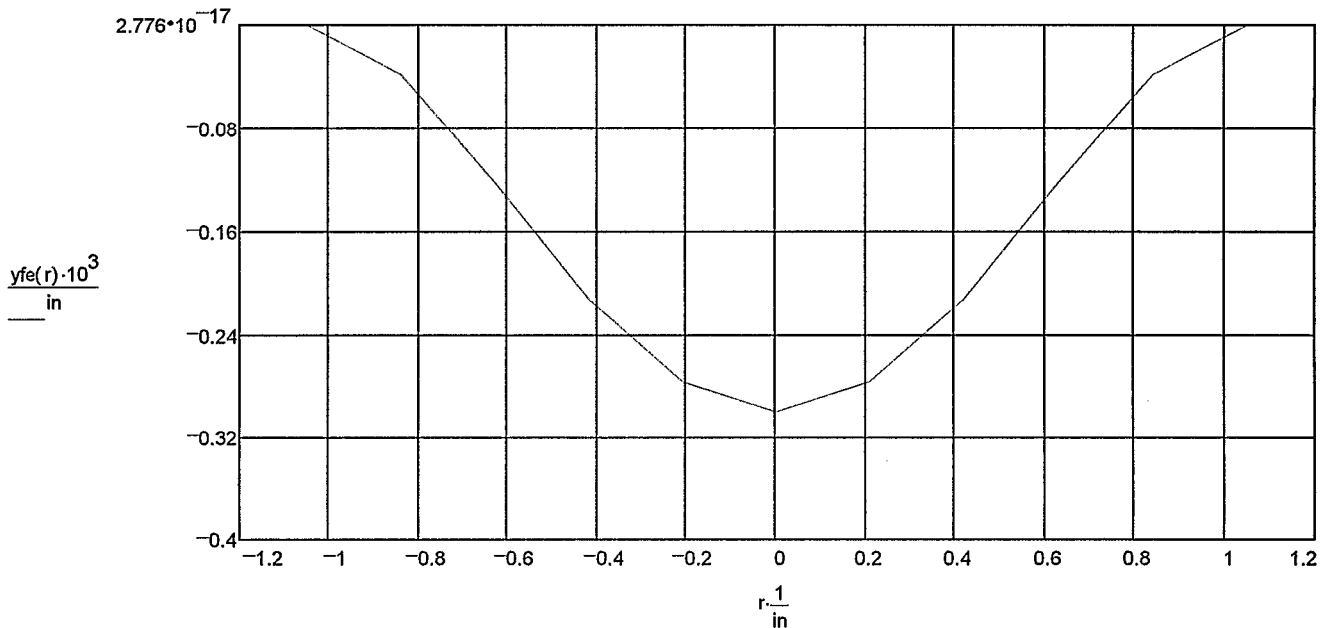
$$\theta_{afe} := 0 \quad *q \quad \theta_{afe} = 0 \quad *q \quad M_{rafe}(q) := \frac{a^2}{8} \cdot -q \quad M_{rafe}(q) = -37.898 \cdot \text{lbf}$$

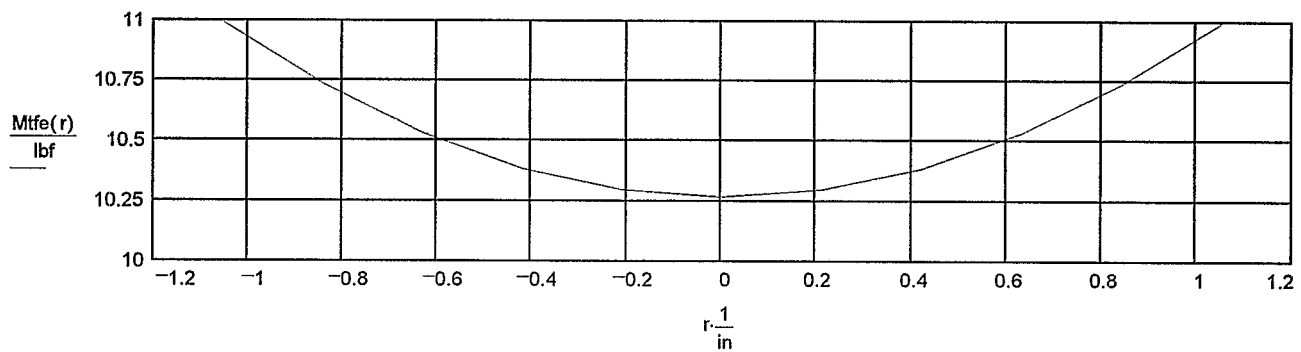
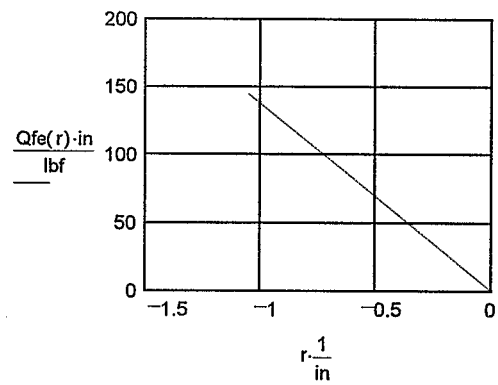
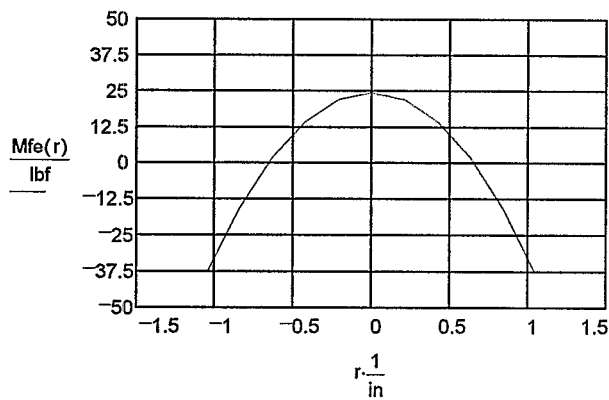
$$Q_{afe} := -\frac{a}{2} \quad *q \quad Q_{afe} = -0.525 \cdot \text{in} \quad *q \quad Q_{afe}(q) := -\frac{a}{2} \cdot q \quad Q_{afe}(q) = -144.375 \cdot \frac{\text{lbf}}{\text{in}}$$

$$y_{fe}(r) := \left(\frac{-a^4}{64 \cdot D} + \frac{a^2 \cdot r^2}{32 \cdot D} - \frac{r^4}{64 \cdot D} \right) \cdot q \quad M_{fe}(r) := \frac{q}{16} \cdot \left[\left[a^2 \cdot (1 + \nu) \right] - \left[r^2 \cdot (3 + \nu) \right] \right] \quad M_{fe}(a) = -37.898 \cdot \text{lbf}$$

$$M_{tfe}(r) := \left[\frac{a^2 \cdot (1 - \nu^2)}{16} - \frac{(1 - \nu^2) \cdot r^2}{16} - \frac{\nu}{16} \cdot \left[\left[a^2 \cdot (1 + \nu) \right] - \left[r^2 \cdot (3 + \nu) \right] \right] \right] \cdot q \quad Q_{fe}(r) := \frac{-q \cdot r}{2}$$

$$r := -a, -a + .21 \cdot \text{in} .. a$$





$$\sigma_{vr}(r) := \frac{M_{fe}(r) \cdot 6}{t^2}$$

$$\sigma_{tvr}(r) := \frac{M_{tfe}(r) \cdot 6}{t^2}$$

$$\epsilon_{tvr}(r) := \frac{\sigma_{tvr}(r)}{E}$$

$$\epsilon_{vr}(r) := \frac{\sigma_{vr}(r)}{E}$$

$$\sigma_{vr}(0 \cdot \text{in}) = 4172 \cdot \text{psi}$$

$$\sigma_{vr}(a) = -6468 \cdot \text{psi}$$

$$\epsilon_{tvr}(0 \cdot \text{in}) = 60.42004 \cdot 10^{-6}$$

$$\epsilon_{tvr}(a) = 64.68 \cdot 10^{-6}$$

$$\sigma_{tvr}(0 \cdot \text{in}) = 1752 \cdot \text{psi}$$

$$\sigma_{tvr}(a) = 1876 \cdot \text{psi}$$

$$\epsilon_{vr}(0 \cdot \text{in}) = 143.85724 \cdot 10^{-6}$$

$$\epsilon_{vr}(a) = -223.03448 \cdot 10^{-6}$$

$$\begin{bmatrix} \sigma_{vr}(.285 \cdot \text{in}) \\ \sigma_{vr}(.205 \cdot \text{in}) \\ \sigma_{vr}(.255 \cdot \text{in}) \\ \sigma_{vr}(.255 \cdot \text{in}) \\ \sigma_{vr}(.84 \cdot \text{in}) \\ \sigma_{vr}(.805 \cdot \text{in}) \\ \sigma_{vr}(.845 \cdot \text{in}) \\ \sigma_{vr}(.875 \cdot \text{in}) \end{bmatrix} = \begin{bmatrix} 3388 \\ 3766 \\ 3544 \\ 3544 \\ -2638 \\ -2082 \\ -2719 \\ -3217 \end{bmatrix} \cdot \text{psi}$$

$$\begin{bmatrix} \epsilon_{vr}(.285 \cdot \text{in}) \\ \epsilon_{vr}(.205 \cdot \text{in}) \\ \epsilon_{vr}(.255 \cdot \text{in}) \\ \epsilon_{vr}(.255 \cdot \text{in}) \\ \epsilon_{vr}(.84 \cdot \text{in}) \\ \epsilon_{vr}(.805 \cdot \text{in}) \\ \epsilon_{vr}(.845 \cdot \text{in}) \\ \epsilon_{vr}(.875 \cdot \text{in}) \end{bmatrix} = \begin{bmatrix} 117 \\ 130 \\ 122 \\ 122 \\ -91 \\ -72 \\ -94 \\ -111 \end{bmatrix} \cdot 10^{-6}$$

$$\begin{bmatrix} \epsilon_{vr}(.285 \cdot \text{in}) \\ \epsilon_{vr}(.205 \cdot \text{in}) \\ \epsilon_{vr}(.255 \cdot \text{in}) \\ \epsilon_{vr}(.255 \cdot \text{in}) \\ \epsilon_{vr}(.84 \cdot \text{in}) \\ \epsilon_{vr}(.805 \cdot \text{in}) \\ \epsilon_{vr}(.845 \cdot \text{in}) \\ \epsilon_{vr}(.875 \cdot \text{in}) \end{bmatrix} \cdot \frac{1}{\epsilon_{vr}(a)} = \begin{bmatrix} -0.524 \\ -0.582 \\ -0.548 \\ -0.548 \\ 0.408 \\ 0.322 \\ 0.42 \\ 0.497 \end{bmatrix}$$

$$\begin{bmatrix} \frac{1}{\epsilon_{vr}(.84 \cdot \text{in})} \\ \frac{1}{\epsilon_{vr}(.805 \cdot \text{in})} \\ \frac{1}{\epsilon_{vr}(.845 \cdot \text{in})} \\ \frac{1}{\epsilon_{vr}(.875 \cdot \text{in})} \end{bmatrix} \cdot \epsilon_{vr}(a) = \begin{bmatrix} 2.452 \\ 3.107 \\ 2.379 \\ 2.011 \end{bmatrix}$$

$$\begin{bmatrix} \frac{1}{\epsilon_{vr}(.285 \cdot \text{in})} \\ \frac{1}{\epsilon_{vr}(.205 \cdot \text{in})} \\ \frac{1}{\epsilon_{vr}(.255 \cdot \text{in})} \\ \frac{1}{\epsilon_{vr}(.255 \cdot \text{in})} \end{bmatrix} \cdot \epsilon_{vr}(0 \cdot \text{in}) = \begin{bmatrix} 1.231 \\ 1.108 \\ 1.177 \\ 1.177 \end{bmatrix}$$

